



ELSEVIER

7 October 1994

**CHEMICAL
PHYSICS
LETTERS**

Chemical Physics Letters 228 (1994) 436-442

Ab initio classical trajectory study of $\text{H}_2\text{CO} \rightarrow \text{H}_2 + \text{CO}$ dissociation

Wei Chen¹, William L. Hase, H. Bernhard Schlegel*Department of Chemistry, Wayne State University, Detroit, MI 48202, USA*

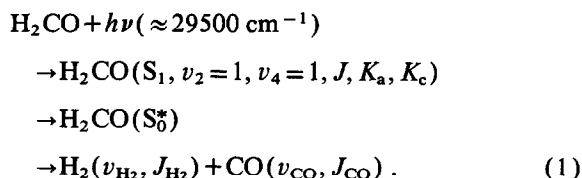
Received 23 May 1994; in final form 29 July 1994

Abstract

Classical trajectories for $\text{H}_2\text{CO} \rightarrow \text{H}_2 + \text{CO}$ dissociation have been calculated directly from ab initio molecular orbital computations at the HF/3-21G and HF/6-31G** levels of theory, without constructing a global potential energy surface. The classical equations of motion were integrated on local fifth-order polynomial surfaces fitted to the energies, gradients and Hessians computed at the beginning and end points of each step along the trajectory. The calculated vibrational and rotational energy distributions and average impact parameter of the products are in very good agreement with experiment. The relative translational energy is higher than experiment because the barrier is overestimated at both levels of theory.

1. Introduction

The photodissociation of formaldehyde has been studied intensively for more than two decades [1-17]. The mechanism of photolysis below the threshold for the radical dissociation channel ($\text{H} + \text{HCO}$), e.g., photolysis of the 2^1A_1 band of S_1 state, is well known [1]



The electronically excited $\text{H}_2\text{CO}(S_1)$ internally converts radiationlessly to highly excited vibrational levels of the ground electronic state (S_0) where it then undergoes unimolecular decomposition over a steep barrier. The activation energy for this reaction is es-

timated to be 79.2 ± 0.8 kcal/mol [2]. Experimental studies of the energy partitioning in the fragments, carried out mainly by Moore and co-workers, include translational energy distribution by time-of-flight (TOF) mass spectrometry [3], CO vibrational and rotational distributions by laser-induced fluorescence (LIF) [4], and H_2 vibrational and rotational distributions by coherent anti-Stokes Raman spectroscopy (CARS) [5,6] and Doppler-resolved LIF [7]. Quantum-state correlations [7] and vector correlations [8,9] have also been carefully investigated. Most recently, results suggest that a second fragmentation path, $\text{H}_2\text{CO} \rightarrow \text{H} + \text{HCO} \rightarrow \text{H}_2 + \text{CO}$, may also be open [10].

Considerable theoretical effort has been spent on finding the properties of the transition state and understanding the molecular dynamics [12-17]. The best predicted barrier height of the reaction is 80.9 ± 3.0 kcal/mol at the MCSCF level [15] and 81.4 kcal/mol at CCSDT-1 level [16]. Miller and co-workers [17] recently carried out classical trajectory studies by using the empirical valence-bond (EVB) model fitted to ab initio results at CCSD/TZ2P and

¹ Current address: Department of Chemistry, Iowa State University, Ames, IA 50011, USA.

MP2/TZP levels of theory. Their calculations with this CCSD/EVB model potential give excellent agreement with experimental data for the product-state distributions of CO and H₂.

The traditional approach to studying reaction dynamics by classical trajectory calculations is to construct an analytical potential energy surface fitted to experimental data and/or ab initio molecular orbital energies [18–20]. Another approach is to use ab initio and semi-empirical molecular orbital calculations directly in classical trajectory studies [21,22] and this has become feasible [23,24] because of advances in computer speed and improvements in molecular orbital software. If analytical first and second derivatives can be computed at a reasonable cost using standard electronic structure methods, the classical equations of motion can be integrated directly on a local quadratic surface for an appropriately small step size. Helgaker, Uggerud and Jensen [23,24] have used this approach to obtain classical trajectories for the elimination of H₂ from H₃ and CH₂OH⁺. Because of the anharmonicity of the potential energy surface, the stepsize for integration on the local quadratic energy surface has to be rather small. In this Letter, we present a new algorithm that employs a fifth-order polynomial model surface fitted to the energies, gradients and Hessians at the beginning and end points of each integration step. The cost for the trajectory calculations is reduced significantly, since considerably larger step sizes can be used without loss of accuracy in the integration of the classical trajectories. The methodology is demonstrated in a study of H₂CO → H₂ + CO calculated at the HF/3-21G and HF/6-31G** levels of theory.

2. Method

Molecular energies, gradients and second derivatives were calculated using the Gaussian series of ab initio molecular orbital programs [25]. The integration of a step along a classical trajectory is divided into two parts. A predictor step is taken by integrating the classical equations of motion from x_i to x'_{i+1} on a local quadratic model using the energy, gradients and second derivatives from the previous ab initio calculation at x'_i , near x_i . A new set of energy,

gradients and second derivatives are calculated at x'_{i+1} and a polynomial surface is fitted to the data at x_i and x'_{i+1} (fifth-order parallel to $x'_{i+1} - x_i$, second order in the perpendicular directions). A corrector step is then taken on the polynomial surface, re-integrating the classical trajectory from x_i to x_{i+1} . The integration time for the step is adjusted to yield a fixed distance between x_i and x'_{i+1} (this distance is analogous to a trust radius used in geometry optimization). A trajectory is terminated when the distance between the fragments is greater than 13 bohr and the gradient for the separation of the fragments is less than 5×10^{-7} hartree/bohr. In the final product analysis, the rotational quantum numbers are obtained by equating the classical and quantum expressions for angular momentum. The vibrational quantum numbers are obtained by integrating the Bohr–Sommerfeld quantization condition using a Morse function fitted to the ab initio potentials for the diatomics.

3. Discussion

In order to simulate the experimental condition of photolysis of the 2¹4¹ band (29500 cm⁻¹), initial conditions were selected as described by Chang et al. [17]. Trajectories were started by adding the corresponding excess energy, 5.1 kcal/mol, to the reaction coordinate at the transition state of H₂CO (note that the barriers computed at HF/3-21G and HF/6-31G** are 25.8 and 26.0 kcal/mol higher than experiment). Zero-point energy was added to each normal mode with a suitable random distribution of initial vibrational coordinates and momenta. The total angular momentum was kept equal to zero, since the initial state of H₂CO(S₁) from the photolysis has a small rotational quantum number (≈ 10) [4–7] and has only a small effect on the fragment rotational and vibrational distributions [4]. A total of 400 trajectories were calculated at both the HF/3-21G and HF/6-31G** levels of theory. With the stepsize of 0.32 $\sqrt{\text{amu bohr}}$, each trajectory runs about 60 steps and requires about 7 min of CPU time for the HF/3-21G calculations and 40 min of CPU time for the HF/6-31G** calculations on an IBM RS/6000 590.

The total translational energy distributions are shown in Fig. 1. Experimentally, the average of the

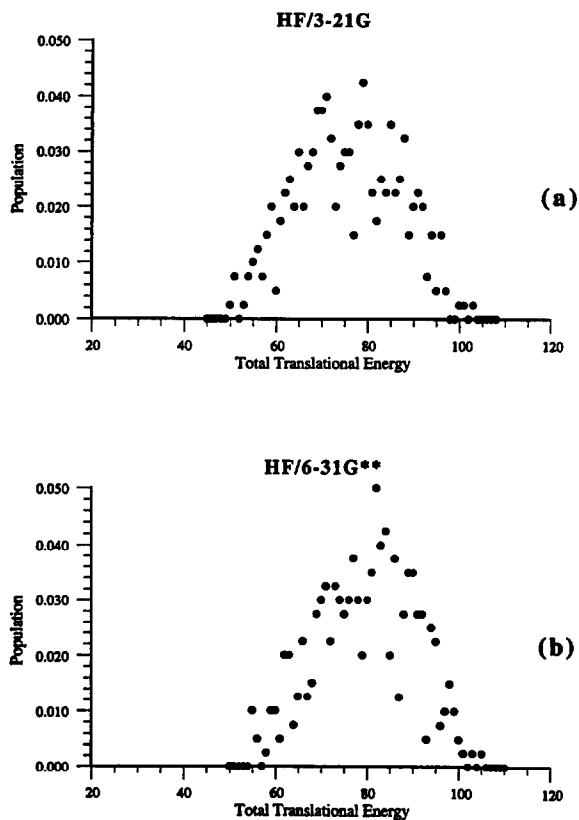


Fig. 1. Total translational energy distributions calculated at (a) the HF/3-21G and (b) the HF/6-31G** levels of theory.

total translational energies is about 55 kcal/mol [3]. For the HF/3-21G and HF/6-31G** calculations, the average of the total translational energies are 75.4 and 79.6 kcal/mol, about 20 and 25 kcal/mol higher than the experimental result, respectively. Since both theoretical levels overestimate the barrier by 26 kcal/mol, it is apparent that most of the excess energy from overestimation of the barrier stays in the translational degrees of freedom. The calculated partitioning of translational energy is in accord with the ratio of the reduced mass of the fragments, i.e. $E_T(\text{H}_2)/E_T(\text{CO}) = \mu_{\text{CO}}/\mu_{\text{H}_2} \approx 13.7$.

Table 1 lists the calculated and observed vibrational distributions for H₂ and CO. For the CO vibrational distribution, both levels of theory show that only the $v=0$ and $v=1$ states are populated, in agreement with the experimental results [4,11]. The calculations give a slightly higher populations for the $v=1$ state (17% and 18% versus 12% for experiment). Since the experimental error bars are 4%, the

calculated data are still in reasonable agreement with experiment. The H₂ vibrational distribution calculated at the HF/3-21G level yields higher populations in high vibrational states than observed experimentally. About 20% of the excess energy due to the overestimation of the barrier appears as H₂ vibrational energy. However, at the HF/6-31G** level the calculated vibrational distribution agrees with the experimental data quite well and has a peak at $v=1$.

The vibrational state correlations between CO and H₂ are found by analyzing the vibrational state population of H₂ as a function of the vibrational state of CO. The results are listed in Table 2. The results at both the HF/3-21G and HF/6-31G** levels of theory show that for $v_{\text{CO}}=1$ the population of high H₂ vibrational states is much less than that for $v_{\text{CO}}=0$. In the HF/6-31G** calculations, for example, the population of $v_{\text{H}_2}=3$ is 43 out of 329 trajectories for $v_{\text{CO}}=0$, but only 2 out of 71 trajectories for $v_{\text{CO}}=1$. Table 3 shows the correlations between translational energies and vibrational quantum numbers. The total translational energy is not affected by v_{CO} but decreases by ≈ 25 kcal/mol as v_{H_2} changes from 0 to 3.

The HF/6-31G** calculated CO rotational distributions for $v_{\text{CO}}=0$ and 1 are shown in Fig. 2; the results for HF/3-21G are similar. The distributions for both levels with $v_{\text{CO}}=0$ are clearly Gaussian-shaped with $\langle J \rangle = 42.8$ and 46.2 and full width at half maximum of 18.2 ± 0.8 and 17.8 ± 1.0 at HF/3-21G and HF/6-31G**, respectively. Although the data for $v_{\text{CO}}=1$ are quite scattered, they still can be fit to a Gaussian with the standard deviations two to three times greater than those of $v_{\text{CO}}=0$. The quantum numbers of the most populated rotational state at the HF/6-31G** are about 4 to 6 quanta higher than experiment ($J=42$). This can be understood in terms of the 'modified impulsive model' [4], since the total available energy is higher in the theoretical calculations. This effect is not as dominant at HF/3-21G because the higher population in the high vibrational states of H₂ reduces the amount of the energy to translation and rotation. The widths of the calculated distributions are a little bit narrower than experiment (22–25) [4].

The calculated rotational distributions for each vibrational state for H₂ are shown in Fig. 3. The peak positions are at $J=3$ for all v_{H_2} at HF/3-21G. At HF/6-31G**, the peak positions are at 2 for $v_{\text{H}_2}=0$, 3 for

Table 1
The vibrational distributions ^a for photofragments CO and H₂

ν	CO			H ₂		
	HF/3-21G	HF/6-31G**	Exp ^b	HF/3-21G	HF/6-31G**	Exp ^c
0	83.2	82.2	88	11.0	22.8	24.2
1	16.8	17.8	12	30.7	36.5	41.3
2				29.5	27.0	24.6
3				21.7	11.2	8.6
4				6.8	2.5	0.3
5				0.3	0.0	0.0

^a In percentage. ^b From Ref. [4]. ^c From Ref. [6].

Table 2
Vibrational correlations ^a between photofragments CO and H₂

	ν_{H_2}						Total
	0	1	2	3	4	5	
HF/3-21G							
$\nu_{\text{CO}}=0$	29	95	99	83	26	1	333
$\nu_{\text{CO}}=1$	15	28	19	4	1	0	67
total	44	123	118	87	27	1	400
HF/6-31G**							
$\nu_{\text{CO}}=0$	65	111	100	43	10	0	329
$\nu_{\text{CO}}=1$	26	35	8	2	0	0	71
total	91	146	108	45	10	0	400

^a Number of trajectories.

Table 3
Averages of total translational energy ^a as function of vibrational quantum numbers

	HF/3-21G	HF/6-31G**
$\nu_{\text{CO}}=0$	75.0	79.2
$\nu_{\text{CO}}=1$	77.4	81.6
$\nu_{\text{H}_2}=0$	90.4	91.5
$\nu_{\text{H}_2}=1$	83.8	83.0
$\nu_{\text{H}_2}=2$	73.1	73.2
$\nu_{\text{H}_2}=3$	64.8	64.8
Total	75.4	79.6

^a In kcal/mol.

$\nu_{\text{H}_2}=1$ and 3, and 4 for $\nu_{\text{H}_2}=2$. Because of the small number of trajectories, it is difficult to compare these results with those from experiment.

The correlation between vibrational and rotational quantum states are shown in Table 4. As seen exper-

imentally, the calculations show that higher vibrational quantum numbers for H₂ are associated with lower rotational quantum numbers for CO. For example, the differences in $\langle J_{\text{CO}} \rangle$ between $\nu_{\text{H}_2}=1$ and 3 are 6.5 and 6.4 at HF/3-21G and HF/6-31G** respectively, which agree with the measured difference of about six quanta [7].

Distributions of the impact parameter, b , are shown in Fig. 4. The average impact parameters are 0.82 and 0.85 Å with full width at half maximum of 0.35 ± 0.01 and 0.33 ± 0.01 Å at HF/3-21G and HF/6-31G**, respectively. These data are in good agreement with the experimental value of about 0.9 Å for an average b [5,6]. The variations in $\langle b \rangle$ with vibrational quantum numbers are listed in Table 5. The impact parameter is not affected significantly by ν_{CO} but decreases slightly with increasing ν_{H_2} .

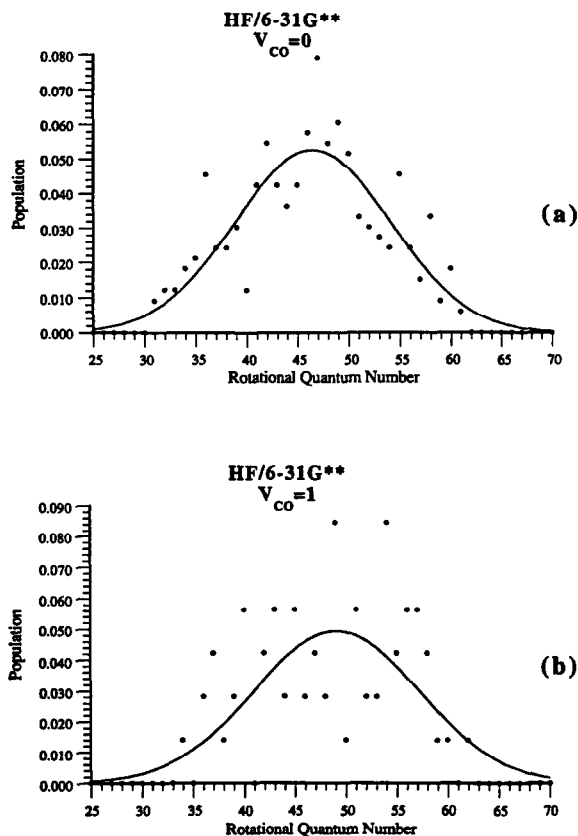


Fig. 2. CO rotational state distributions at the HF/6-31G** level of theory in the CO vibrational quantum state $\nu_{\text{CO}}=0$ (a) and $\nu_{\text{CO}}=1$ (b).

4. Conclusions

This study has illustrated the feasibility of using ab initio classical trajectories to investigate product energy partitioning in the unimolecular dissociation of polyatomic molecules. A new fifth-order polynomial model was developed, which allows the integration stepsize to be increased and, thus, reduces the required computer time. The trajectories are initiated at the potential barrier to mimic experimental conditions and the effect of the exit channel potential on the product energy partitioning [26–29] can be investigated. Previous studies [30] have indicated that trajectories give accurate and valuable information for such direct dissociation processes where problems associated with unphysical zero-point energy flow [31–35] are of no or minor importance.

In the ab initio trajectory calculations presented

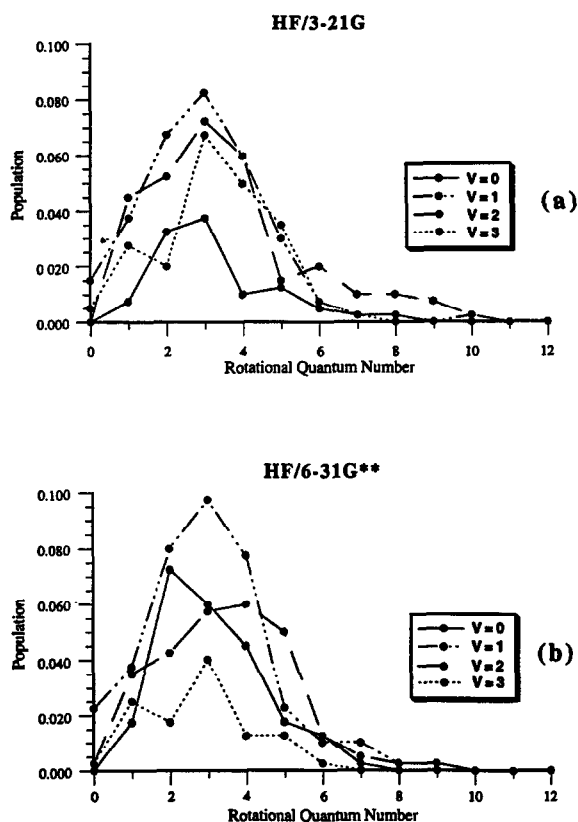


Fig. 3. H₂ rotational state distributions at (a) the HF/3-21G and (b) the HF/6-31G** levels of theory in the various CO vibrational quantum states.

here, the HF/3-21G and HF/6-31G** levels of theory are used to determine the product energy distribution for $\text{H}_2\text{CO} \rightarrow \text{H}_2 + \text{CO}$ dissociation. These theories overestimate the potential barrier by 26 kcal/mol. However, most of the excess energy from the overestimated barrier goes to product translation and the calculated product vibrational and rotational energies are in good agreement with experiment. For the HF/6-31G** calculations, this agreement is near quantitative. Calculated correlations between vibrational and rotational states agree with experiment, as does the calculated distribution of the product impact parameter. Thus, the HF level of theory appears to describe accurately all experimentally measured properties of $\text{H}_2\text{CO} \rightarrow \text{H}_2 + \text{CO}$ dissociation except for product translational energy. The overestimation of the potential energy barrier by HF theory only affects this latter property and the HF theory apparently de-

Table 4

Averages of rotational quantum numbers as a function of vibrational quantum number

	J_{CO}		J_{H_2}	
	HF/3-21G	HF/6-31G**	HF/3-21G	HF/6-31G**
$\nu_{\text{CO}}=0$	42.8	46.2	3.3	3.2
$\nu_{\text{CO}}=1$	44.3	48.4	2.6	2.5
$\nu_{\text{H}_2}=0$	48.8	51.5	3.2	3.1
$\nu_{\text{H}_2}=1$	45.8	47.5	3.0	3.0
$\nu_{\text{H}_2}=2$	42.4	44.1	3.6	3.5
$\nu_{\text{H}_2}=3$	39.3	41.1	3.2	2.7
total	43.1	46.6	3.2	3.1

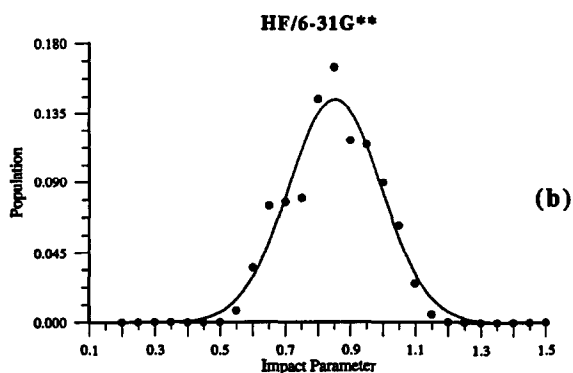
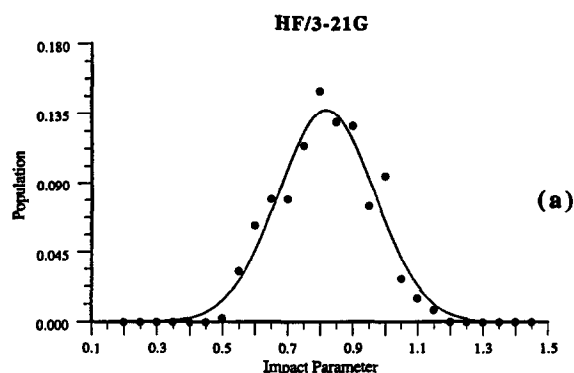


Fig. 4. Impact parameter distribution calculated at (a) the HF/3-21G and (b) the HF/6-31G** levels of theory.

describes the remaining properties of the exit channel potential to give accurate product rotational and vibrational energies.

Table 5

Averages of calculated impact parameters $\langle b \rangle^a$

	HF/3-21G	HF/6-31G**
$\nu_{\text{CO}}=0$	0.817	0.847
$\nu_{\text{CO}}=1$	0.816	0.861
$\nu_{\text{H}_2}=0$	0.856	0.879
$\nu_{\text{H}_2}=1$	0.823	0.843
$\nu_{\text{H}_2}=2$	0.826	0.840
$\nu_{\text{H}_2}=3$	0.790	0.826
total	0.817	0.850

^a In Å.

Acknowledgement

This work was supported by grants from the National Science Foundation (CHE 9400678 and CHE 9023391).

References

- [1] C.B. Moore and J.C. Weisshaar, *Ann. Rev. Phys. Chem.* 34 (1983) 525.
- [2] W.F. Polik, D.R. Guyer and C.B. Moore, *J. Chem. Phys.* 92 (1990) 3453.
- [3] P. Ho, D.J. Bamford, R.J. Buss, T.T. Lee and C.B. Moore, *J. Chem. Phys.* 76 (1982) 3630.
- [4] D.J. Bamford, S.V. Filseth, M.F. Foltz, J.W. Hepburn and C.B. Moore, *J. Chem. Phys.* 82 (1985) 3032.
- [5] M. Péalat, D. Debarre, J.-M. Marie, J.-P.E. Taran, A. Tramer and C.B. Moore, *Chem. Phys. Letters* 98 (1983) 299.
- [6] D. Debarre, M. Lefebvre, M. Péalat, J.-P.E. Taran, D.J. Bamford and C.B. Moore, *J. Chem. Phys.* 83 (1985) 4476.
- [7] T.J. Butenhoff, K.L. Carleton and C.B. Moore, *J. Chem. Phys.* 92 (1990) 377.
- [8] K.L. Carleton, T.J. Butenhoff and C.B. Moore, *J. Chem. Phys.* 93 (1990) 3907.

- [9] T.J. Butenhoff, K.L. Carleton, R.D. van Zee and C.B. Moore, *J. Chem. Phys.* 94 (1990) 1947.
- [10] R.D. van Zee, M.F. Foltz and C.B. Moore, *J. Chem. Phys.* 99 (1993) 1664.
- [11] P.L. Houston and C.B. Moore, *J. Chem. Phys.* 65 (1976) 757.
- [12] M.J. Frisch, R. Krishnan and J.A. Pople, *J. Phys. Chem.* 85 (1981) 1467.
- [13] J.D. Goddard, Y. Yamaduchi and H.F. Schaefer III, *J. Chem. Phys.* 75 (1981) 3459.
- [14] M.J. Frisch, J.S. Binkley and F. Schaefer III, *J. Chem. Phys.* 81 (1984) 1882.
- [15] M. Dupuis and W.A. Lester Jr., B.H. Lengsfeld III and B. Liu, *J. Chem. Phys.* 79 (1983) 6167.
- [16] G.E. Scuseria and H.F. Schaefer III, *J. Chem. Phys.* 90 (1989) 3629.
- [17] Y. Chang, C. Minichino and W.H. Miller, *J. Chem. Phys.* 96 (1992) 4341.
- [18] W.L. Hase, G. Mrowka, R.J. Brudzynski and C.S. Sloane, *J. Chem. Phys.* 69 (1978) 3548.
- [19] R.J. Duchovic, W.L. Hase and H.B. Schlegel, *J. Phys. Chem.* 88 (1984) 1339.
- [20] S.R. Vande Linde and W.L. Hase, *J. Phys. Chem.* 94 (1990) 2778.
- [21] I.S.Y. Wang and M. Karplus, *J. Am. Chem. Soc.* 95 (1973) 8160.
- [22] C. Leforestier, *J. Chem. Phys.* 68 (1978) 4406.
- [23] T. Helgaker, E. Uggerud and H.J.A. Jensen, *Chem. Phys. Letters* 173 (1990) 145.
- [24] E. Uggerud and T. Helgaker, *J. Am. Chem. Soc.* 114 (1992) 4265.
- [25] M.J. Frisch, G.W. Trucks, M. Head-Gordon, P.M.W. Gill, J.B. Foresman, M.W. Wong, B.G. Johnson, H.B. Schlegel, M.A. Robb, E.S. Replogle, R. Gomperts, J.L. Andres, K. Raghavachari, J.S. Binkley, C. Gonzalez, R.L. Martin, D.J. Fox, D.J. DeFrees, J. Baker, J.J.P. Stewart and J.A. Pople, GAUSSIAN 92 (Gaussian Inc., Pittsburgh, PA, 1992).
- [26] J.M. Farrar and Y.T. Lee, *J. Chem. Phys.* 65 (1976) 1414.
- [27] G. Worry and R.A. Marcus, *J. Chem. Phys.* 67 (1977) 1636.
- [28] S. Kato and K. Morokuma, *J. Chem. Phys.* 73 (1980) 3900; 74 (1981) 6285.
- [29] W.L. Hase, D.G. Buckowski and K.N. Swamy, *J. Chem. Phys.* 87 (1983) 2754.
- [30] A. Untch, R. Schinke, R. Cotting and J.R. Huber, *J. Chem. Phys.* 99 (1993) 9553.
- [31] W.L. Hase and D.G. Buckowski, *J. Comput. Chem.* 3 (1982) 335.
- [32] D.-h. Lu and W.L. Hase, *J. Chem. Phys.* 89 (1988) 6723.
- [33] J.M. Bowman, B. Gazdy and Q. Sun, *J. Chem. Phys.* 91 (1989) 2859.
- [34] W.H. Miller, W.L. Hase and C.L. Darling, *J. Chem. Phys.* 91 (1989) 2863.
- [35] G.H. Peslherbe and W.L. Hase, *J. Chem. Phys.* 100 (1994) 1179.